Available online at www.sciencedirect.com

ScienceDirect

Procedia Structural Integrity 43 (2023) 294–299

Structural Integrity Procedia

www.elsevier.com/locate/procedia

10th International Conference on Materials Structure and Micromechanics of Fracture

Effect of Internal Pressure on Microstructural and Mechanical Properties of X10CrNiCuNb18-9-3 (SUPER 304H) Austenitic Stainless Steel

Lucie Pilsová[a,b,*], Marie Ohanková[a], Vladimír Mára[b], Jan Krčil[b], Jakub Horváth[b]

[a]*UJP PRAHA a.s., Nad Kamínkou 1345, 156 10 Prague – Zbraslav, Czech Republic*
[b]*Czech Technical University in Prague, Faculty of Mechanical Engineering, Department of Materials Engineering, Karlovo náměstí 13, 120 00 Prague, Czech Republic*

Abstract

Despite the current tendencies towards decarbonization of the energy sector, it is still necessary to maintain the lifetime of existing coal-fired power plants. Austenitic stainless steels belong among materials used in energetics, in this case, SUPER 304H (X10CrNiCuNb18-9-3). This steel is used for the experiment that simulates real operating conditions, specifically high temperature (700 °C) and constant inner pressure (25 MPa), which is induced by inserting a distilled water medium before sealing. This work deals with the evaluation of the microstructure and mechanical properties of the SUPER 304H specimens, both with and without inner pressure. All the specimens underwent the same long-term exposure in a form of laboratory annealing. The mechanical properties were evaluated by performing the tensile, impact and hardness tests and microstructure was characterized by light optical microscopy and scanning electron microscopy.

Keywords: Austenitic stainless steel; microstructure; reheaters; superheaters; internal pressure.

* Corresponding author. Tel.: +420-22435-7249.
E-mail address: lucie.pilsova@fs.cvut.cz

10.1016/j.prostr.2022.12.274

1. Introduction

The supercritical and ultra-supercritical boilers in conventional powerplants meet the efficiency requirements but the materials are close to the applicability limits. This is also a case of the SUPER304H steel which was used as a material on the retrofitted blocks in fossil fuel power plants along with the construction of the new facilities. SUPER304H steel belongs to the group of high alloyed austenitic stainless steels. It has a great oxidation and creep stability in comparison with older AISI 304H steel, also it does not contain delta ferrite that is often in the operation conditions a suitable nucleation site of the brittle phases and precipitates leading to the deterioration of the mechanical properties. There have been many articles discussing this material's behavior in high temperature conditions, Le et al. (2020) and creep testing after long-term service, Zieliński et al. (2022). This work outlines a new approach of testing these materials using the specimens with induced internal pressure.

2. Materials and methods

The experimental material consists of the reheater tubes made of SUPER304H austenitic stainless steel. Sealing caps of the experimental specimen were made of martensitic P91 and austenitic AISI 310 steels. The weld joint was prepared using TIG method with high-alloyed Ni-based UTP A 6170 Co filler material. The nominal composition of the used tubes and the filler material according to the Böhler (2015) is shown in Table 1.

Table 1. Nominal composition of experimental materials (wt. %)

Material	C	Si	Mn	P	S	Cu	Cr	Ni	Nb	N	Al	V	Mo	Co	Ti	Fe
SUPER304H	0.03	< 0.3	<1.0	<0.40	< 0.010	3.0	18.0	9.0	0.45	0.85	---	---	---	---	---	bal
AISI 310	< 0.25	< 1.5	<2.0	< 0.045	< 0.030	---	25.0	20.5	---	---	---	---	---	---	---	bal
P91	< 0.12	< 0.5	0.45	< 0.02	< 0.005	< 0.3	8.8	< 0.3	0.08	---	< 0.04	0.2	---	---	---	bal
UTP A 6170 Co	0.06	< 0.3	---	---	---	---	22.0	bal.	---	---	1.00		8.5	11.5	0.4	1

The tubes were cut using LECO MSX255 metallographic cutting machine and mounted in Technotherm3000 conductive powder in the LECO MX400 automatic mounting press. The samples were mechanically ground (ending at grit P4000) and polished with 0.05 μm Al_20_3 suspension. For the EBSD analysis samples was used electrolytic polishing using an automatic DC power source Struers Lectropol with electrolyte 1:9 perchloric acid:acetic acid and setup: flowrate 20 l/s, 16 V, 5 s. For the LOM observation, the samples in as received state were electrolytically etched in 10% aqueous solution of oxalic acid (DC Source Struers Lectropol, external etching, 25 V, 10 s). The samples after long-term annealing were electrolytically etched in electrolyte consisting of 20% aqueous NaOH (DC Source Struers POLIPOWER, 1.5 V, 2 s)

LOM images were taken using microscopes Neophot32 Karl Zeiss and Olympus DSX1000. SEM was performed using the Jeol JSM-7600F scanning electron microscope equipped with detectors for EDS (Oxford X-Max 50 mm^2 and EBSD (HKL Nordlys). The results of the EBSD analysis in the IPF map were processed using the ATEX software, Beausir and Fundenberger, 2017. HV10 hardness measurement was done using an automated hardness tester Struers Duramin 40 AC3 equipped with a Vickers indenter. Tensile testing at room temperature was carried out with the Instron 5800R Tensile and Compression Test System with constant crosshead speed v = 0.5 mm/s equipped with video extensometer AVE2. The Charpy Impact test was performed using VEB WPM 300 J pendulum. The tube specimens were long-term aged in a resistance furnace at 700 °C for 3,744 and 10,000 h, respectively, in the air atmosphere. The temperature was continuously checked with a type K thermocouple placed in the center of the furnace chamber.

3. Experiment

The experimental specimens were made of the reheater tubes (outer diameter OD = 38 mm, wall thickness t = 6.3 mm) and sealed on both sides with a welded cap. One side was designed with a hole to inject the distilled water medium. The injection hole was then also sealed, and the weld joints were checked by means of non-destructive

testing. Specimens were placed in an electrical resistance furnace and heated to 700 °C. The inner pressure of the steam in the sealed tube was calculated to be 25 MPa. At this time, two samples after long-term annealing were evaluated. One after 3,744 h and second after 10,000 hours.

Fig. 1. Tube specimen with welded caps, state after long-term annealing

The two tube specimens were before and after placing in the furnace scanned with laser 3D scanner. This was planned to observe, whether here would be any change in overall shape caused by the inner pressure. Each tube also carried a reference ring-shaped sample, which was destined for the microstructural state comparison. SUPER304H steel shows certain changes in microstructure after longer exposition to higher temperature (approximately 600 °C) – significant precipitation of carbides and formation of Cr-based intermetallics at grain boundaries. Because of this, the effect of inner pressure on the possible microstructural changes deemed to be of interest as well.

4. Results

All the specimens underwent long-term exposure in a form of laboratory annealing for 3,744 h and 10,000 h respectively. Subsequently, the samples were weighed, measured and 3D scanned for further investigation. For the following testing, the tube was cut into sections destined for the tensile test and Charpy test specimens manufacturing and the middle part was used for the microstructure examination. The assumption was that there would be the greatest change in size and in the effect of internal pressure.

4.1. Mechanical testing

The results of the tensile test showed an increase in the tensile strength, starting at 590±40 MPa in case of the base material and continuing to (697±14) MPa after 10,000 h in the furnace. However, with this strengthening the ductility $A_{5.65}$ showed no measurable decrease – with the values lying in the standard deviation limits, (51±3) % in the case of the base material, and (49±1) % in the case of the 10,000 h of aging. More significant decrease was observed among the Charpy V-Notch Test. The initial absorbed energy KV 300/5 of the subsize specimens was 93±5 J and then fell by 50 % after 3,744 h and by 70 % to (26±2) J after 10,000 h exposure. The initial hardness of the as-state was (173±4) HV10 and (188±2) HV10 after 10,000 h respectively.

4.2. Microstructure

The as-received material consists of austenitic grains with twins and evenly dispersed particles of Nb(C,N) also rich in Mo. In the longitudinal section the Nb(C,N) particles tend to form bands in the direction of the manufacturing rolling process. In the long-term aged material, there can be seen particles rich in Cr on the grain boundaries (probably MX and $M_{23}C_6$ carbides) and on the grain boundary triple junctions the sigma phase. Its presence was indicated by selective etching and confirmed using EBSD (Fig. 2c) and EDXS mapping (Fig. 3).

4.2.1. Light optical microscopy

The as-received state of the SUPER304H steel is shown in Fig. 2a. The chemical resistance is high; therefore, the etching is often uneven. On the other hand, the more long-term aged material, the more sensitized grain boundaries and thus revealing microstructure easier. For the area fraction determination of the brittle sigma phase was used

electrolytic etching in aqueous 20 % NaOH electrolyte (Fig. 2b). The area fraction of the intermetallics (after 10,000h) was 2.5±0.5 % and by the reference sample 2.2±0.3 %. In the center of the wall thickness the sigma phase particles' distribution is uniform. Due to the oxidation of the inner and outer surface, the matrix is depleted of Cr, which forms the oxidic layers on the interface. Near the surface of the tube there is no such significant precipitation of the sigma phase (in the case of the pressure specimen - outer edge approx. 150 µm, inner surface of 100 µm). Sigma phase-free area is more pronounced in the pressure sample at the outer edge where the sample is in contact with the furnace atmosphere.

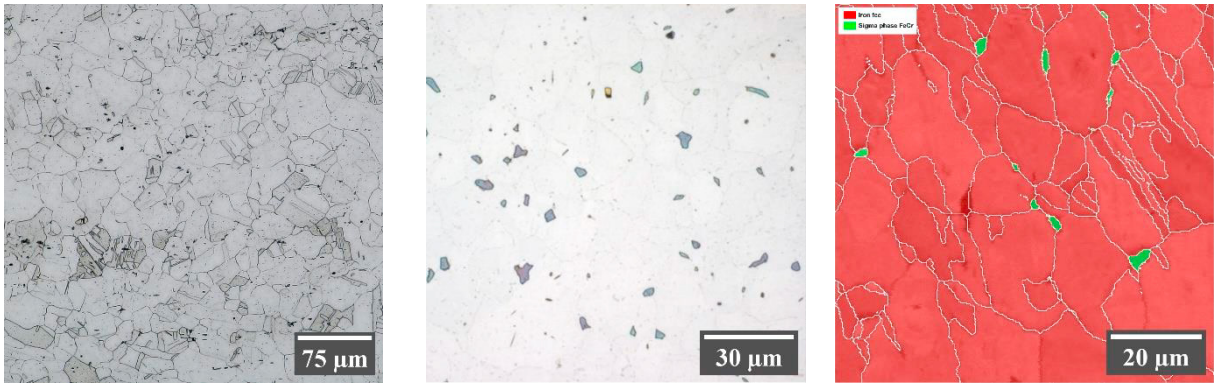

Fig. 2. (a) as-received state; (b) selective etching, 10,000 h specimen; (c) EBSD phase map, specimen after 10,000 h at 700 °C

4.2.2. Scanning Electron Microscopy – Microstructure

The typical case of precipitation of Cr particles (chain-like carbides) at grain boundaries is shown in Fig. 3. Primary particles rich in Nb are often cracked due to rolling production technology. The intermetallic sigma phase often occurs in these places, most noticeable after exposure for 10,000 hours.

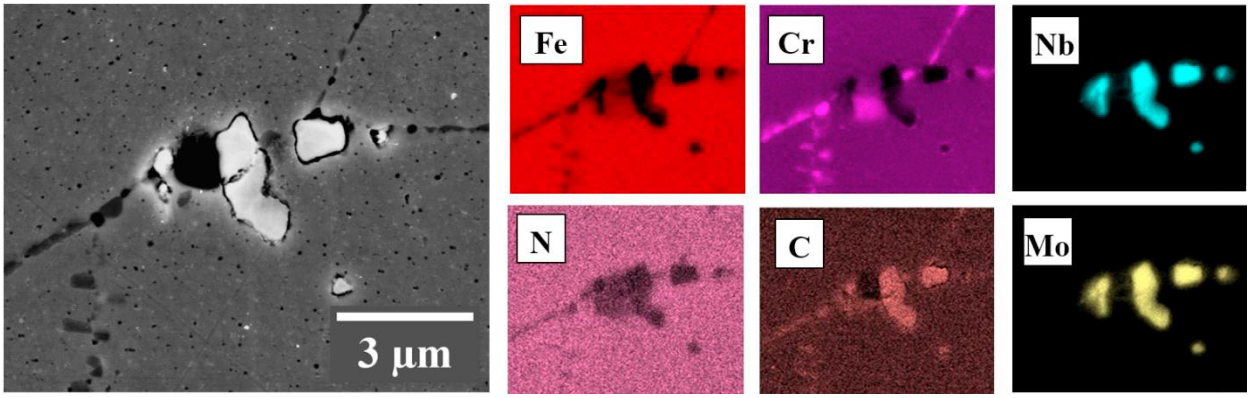

Fig. 3. EDXS map of particles at the grain boundaries (state after 10,000 h and 700 °C)

4.2.3. Scanning Electron Microscopy - Fractography

The basic macroscopic analysis showed the presence of cup and cone tensile fracture of cylindrical specimens after uniaxial tensile test, which is typical for ductile metals. SEM fracture surface analysis confirmed presence of characteristic morphologic features of transcrystalline ductile fracture with dimple morphology. Ductile tearing,

dimple rupture and coalescence of microvoids (see Fig. 4a) can be observed across the fracture surface. The coalescence of microvoids (see Fig. 4b) occurs predominantly at the grain boundaries, where the small chromium-based particles are present and in the center of the equiaxed dimples with size of approx. 10 μm, cleavage planes can be observed near the ruptured brittle particles (see Fig. 4c). Same behavior was observed on the fracture surface of impact test specimens.

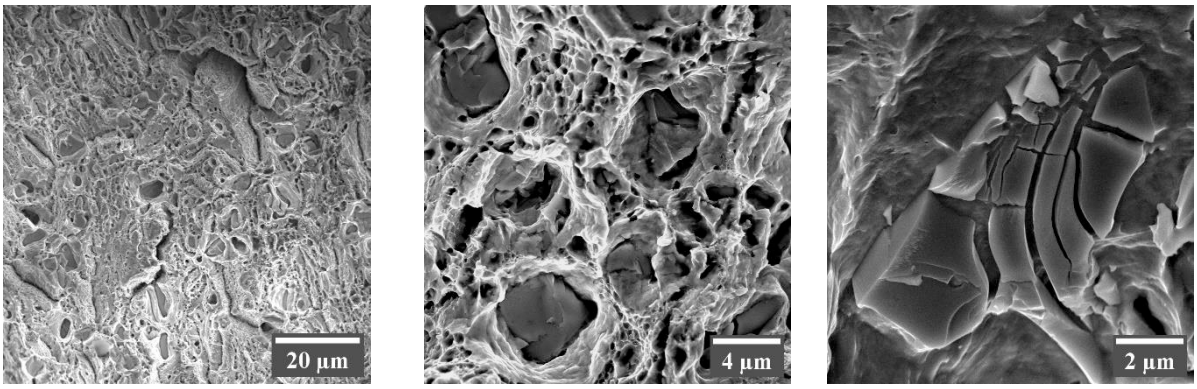

Fig. 4. SEM fractographic analysis: (a) fracture surface overview, (b) detail of ductile fracture with dimples and particles, (c) cleavage facets near the ruptured particle

EDXS mapping shows the area of the ruptured particle which is rich on Cr containing also Fe. This sigma phase particle is accompanied by the smaller ones, Nb and Mo primary carbonitrides.

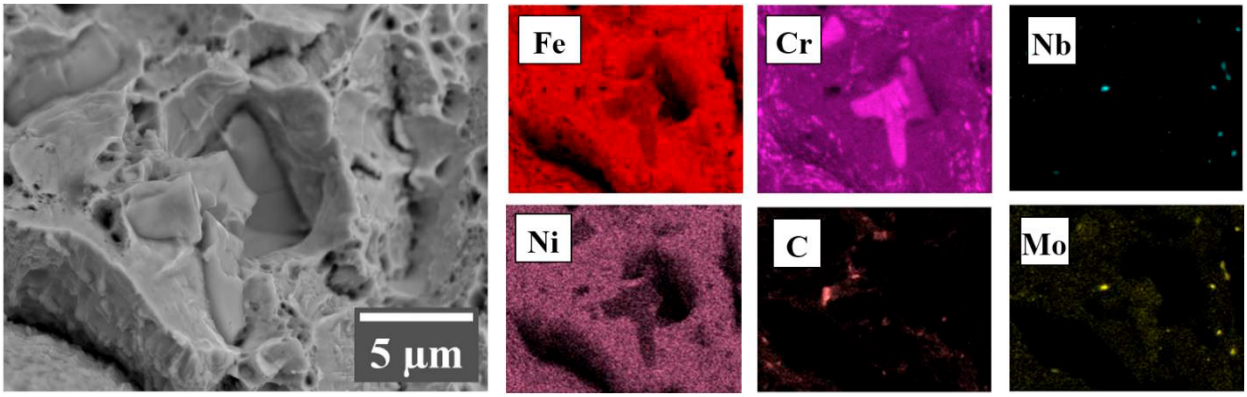

Fig. 5. EDXS map of the tensile specimen fracture area (state after 10,000 h and 700 °C)

5. Discussion

The sealed and water-filled tube specimens were annealed at 700 °C for 3,744 and 10,000 hours. The elevated temperature caused the transformation of specific amount of water into the vapor with pressure of 25 MPa. Sealed specimens were checked by ultrasonic thickness gauge. Since there was no pronounced inflation of specimen, it is not possible to unequivocally declare/state that specimens have changed their shape. The ambiguity of the shape-

change is further emphasized by both manufacturing tolerances of a wall thickness and the surface oxidation during the experiment.

Results of mechanical testing are clearly showing that the microstructural changes are causing the hardening of material. However, the increase of hardness and tensile strength is accompanied by the severe decrease of ductility. This was proven by the impact test where the absorbed energy decreased from initial value (93±5) J to (26±2) J. The observation of fracture areas confirmed presence of transcrystalline ductile fracture with dimple morphology. Furthermore, the conjunction of micro-voids with cracked particles was observed. These particles were, in this case, identified as a type of the sigma phase containing predominantly Fe and Cr, accompanied by the presence of Si and Mn. The identification was done by EDXS and EBSD methods. This type of behavior is however also common for specimens without inner pressure as i.e., presents Nam et al. (2017). The thinner oxide layer on the inner surface of the specimen together with smaller Cr-depleted area bellow the inner surface were sole substantial differences when compared to specimens without inner pressure.

The subject of further investigation should be the monitoring of inner pressure values and possibility of the inner pressure increase for the following experiments.

6. Conclusions

Previously discussed results can be summarized into following conclusions:

- The long-term annealing at 700 °C resulted in expected changes in the SUPER304H steel microstructure (precipitation on grain boundaries) following with a slight hardness and tensile strength increase, but with a dramatic decrease in absorbed energy.
- The microstructure of the reference sample (without inner pressure) looks the same according to the used methods. The difference can be seen in the microstructure near inner and outer specimen surface. While the reference sample has Cr-depleted areas in the same depth (approximately 150 μm), the pressure specimen has this area shorter (100 μm in depth) in the inner surface. This leads to the conclusion that the oxidation in the internal environment of the pressure sample proceeds more slowly.
- The available methods have shown that the internal pressure of 25 MPa does not significantly contribute to changes in the microstructure caused by elevated temperature. It leaves for the further investigation to increase the pressure conditions in the sample.

Acknowledgements

This paper was supported by the Ministry of Industry and Trade of the Czech Republic, project no. FV40166 and by the Technology Agency of the Czech Republic, project no. TH01020160.

References

B. Beausir, J.-J. Fundenberger, Analysis Tools for Electron and X-ray Diffraction, Université de Lorraine, Metz, 2017. www.atex-software.eu.

Böhler Schweisstechnik Deutschland, Welding Guide, (2015). https://westec.al/wp-content/uploads/2015/03/UTPHandbook.pdf.

T.G. Le, K.B. Yoon, Y.W. Ma, Metal Temperature Estimation and Microstructure Evaluation of Long-Term Service-Exposed Super304H Steel Boiler Tubes, Metals and Materials International. (2020). https://doi.org/10.1007/s12540-020-00808-4.

K.G. Nam, Y.S. He, J.C. Chang, Microstructural Evolution of Super304H Steel upon Long-Term Aging, Key Engineering Materials. 727 (2017) 36–42. https://doi.org/10.4028/www.scientific.net/KEM.727.36.

A. Zieliński, R. Wersta, M. Sroka, The study of the evolution of the microstructure and creep properties of Super 304H austenitic stainless steel after aging for up to 50,000 h, Archives of Civil and Mechanical Engineering. 22 (2022) 89. https://doi.org/10.1007/s43452-022-00408-6.